ADRC speed Control of IPMSM with Current Regulator

Wen Jianping, Zhang Xuhui

***Abstract*—This paper introduces the novel current control strategy of interior permanent synchronous motor (IPMSM). The current control scheme consists of the improved auto disturbance rejection control current regulator and the modified transition rules. The decoupling, linearizing and anti-windup control is realized simultaneously by disposing the cross-coupling effects as the disturbances. Combining the modified transition rules with the reference output voltage of the current regulator, the smooth transitions are achieved when the different control modes are switching. Test results are given to verify the validity of the proposed method.**

***Index Terms*—Anti-windup control, auto disturbance rejection control (ADRC), decoupling control, interior permanent magnet synchronous motor (IPMSM).**

I. INTRODUCTION

IPMSM is widely used in many industrial applications due to its high efficiency, high power density and particularly magnetic saliency increasing the power capability [1]-[3]. IPMSM drive is required to offer high efficiency operation over wide-speed ranges and fast torque response [4]. In [5], a linear torque control strategy is used to utilize the reluctance torque and extend the maximum torque per ampere (MTPA) control in the constant torque region up to the entire field-weakening region i.e. constant power region. The both regions are separated according to the rotor speed. The change between the MTPA control and the field-weakening control is determined according to the rotor speed and virtual control bound. The current control, however, using conversional Proportional-integral (PI) control exists the cross-coupling effects and windup phenomenon. The fast dynamic response is poor. In [6], the high-performance current controller using the feedforward compensation PI regulator and voltage command compensation is proposed to improve the torque response. A nonlinear control ensuring maximum efficiency is proposed in [7] which cancelled the saturation dependent parameters such as d- and q-axis inductances and armature reaction dependent magnet inductances. In [8]-[11], from the viewpoint of windup produced by the integral term in the PI current controller, the new field-weakening control is proposed to improve the toque response. The disadvantages of PI controllers limit the performance of the current regulation for IPMSM drive. Based on the conventional proportional-integral-derivative control technique, modern control theory and nonlinear control mechanisms, auto disturbance rejection control (ADRC) theory is developed [12]-[13].

This paper presents a novel discrete-time ADRC-based current controller and the transition rules. The ADRC current regulator is used to cancel the cross-coupling terms between d- and q-axis currents. By using the dynamic real-time feedbacks, the ADRC current regulator converts the nonlinear current model into linear one and eliminates the integrator and achieves the anti-windup control. Combining with the output of the ADRC current regulator, the modified transition rules uses the voltage modulation index to choose the control modes and achieve the smooth transition. The proposed method is used over the entire speed range.

Wen Jianping, School of Mechanical Engineering, Xi'an University of Science and Technology, xi'an, China, and Key Laboratory of Expressway Construction Machinery, Chang'an University, xi'an, China.

Zhang Xuhui, School of Mechanical Engineering, Xi'an University of Science and Technology, xi'an, China.

This study is supported by the Key Laboratory of Express-way Construction Machinery (Chang'an University), Shaanxi province, no. 310825151135.

II. ADRC CURRENT CONTROL

A. Mathematical model of IPMSM

On the basis of assumptions that the stator windings generates sinusoidal magnetic field, air gap is uniform and saturation is negligible. With reference to synchronous rotating reference frame, the voltage and torque equations of an IPMSM may be expressed as follows:

$$\begin{bmatrix} u_d \\ u_q \end{bmatrix} = \begin{bmatrix} R_s + pL_d & -\omega_r L_q \\ \omega L_d & R_s + pL_q \end{bmatrix} \begin{bmatrix} i_d \\ i_q \end{bmatrix} + \begin{bmatrix} 0 \\ \omega_r \varphi_f \end{bmatrix} \tag{1}$$

$$T_e = P_n \varphi_f i_q + P_n (L_d - L_q) i_d i_q \tag{2}$$

where, i_d and i_q are *d*- and *q*-axis currents; *p* equals *d/dt*; u_d and u_q are *d*- and *q*-axis voltages; L_d and L_q are *d*- and *q*-axis inductances; R_s is resistance of the stator windings; φ_f is amplitude of the flux; P_n is Number of pole pairs; T_e is electromagnetic torque; ω_r is angular speed of the motor.

The steady-state *d*- and *q*- axis voltage equations can be simplified from **Error! Reference source not found.** as follows:

$$u_{ds} = R_s i_d - \omega_r L_q i_q \tag{3}$$

$$u_{qs} = R_s i_q + \omega_r \left(L_d i_d + \varphi_f \right) \tag{4}$$

For voltage-source-inverter-fed IPMSM drive, there exists an inverter output voltage limit and an output current limit. These constraints can be expressed as

$$I_s = \sqrt{i_d^2 + i_q^2} \le I_{sm} \tag{5}$$

$$U_s = \sqrt{u_d^2 + u_q^2} \le U_{sm} \tag{6}$$

where I_{sm} and U_{sm} are the maximum output current of the inverter and the maximum phase voltage.

when $\omega_r \le \omega_{base}$, the maximum torque can be derived through the MTPA control strategy. For $\omega_r > \omega_C$, the maximum torque per ampere trajectory and voltage limit ellipse have not an intersection point. When $\omega_{base} < \omega_r \le \omega_C$, called first field-weakening region.

When *d*- and *q*- axis currents are equal to zero, one can obtain the corresponding angular speed, ω_C :

$$\omega_C = \frac{U_{sm}}{\varphi_f} \tag{7}$$

B. ADRC

The ADRC consists of the tracking differentiator (TD), the nonlinear state error feedback (NLSEF), the extended state observer (ESO) [14], as shown Fig. 2. v is input signal; y is output signal; e_0 is error integral signal; e_1 is error signal; e_2 is error differential signal; u is controlled input; v_1 can approximate the input signal; v_2 is the differential signal of input signal; b is system parameter. z_1 and z_2 are observation of v_1 and v_2. z_3 is the disturbance observer.

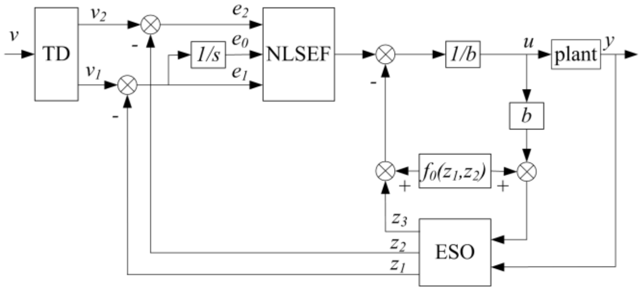

Fig. 1 the block diagram of ADRC

C. ADRC current regulator

From **Error! Reference source not found.**, the *d*- and *q*-axis current mathematical models of IPMSM in the *d-q* reference frame is rewritten:

$$\begin{cases} \dot{i}_d = -\dfrac{R_s}{L_d} i_d + \dfrac{\omega_r L_q}{L_d} i_q + \dfrac{u_d}{L_d} \\ \dot{i}_q = -\dfrac{R_s}{L_q} i_q - \dfrac{\left(L_d i_d + \varphi_f\right)\omega_r}{L_q} + \dfrac{u_q}{L_q} \end{cases} \tag{8}$$

Let cross-coupling terms as the system uncertainties, the second-order ESO for i_d is constructed as follows:

$$\begin{cases} e_d = z_{d1} - i_d \\ \dot{z}_{d1} = f_d + z_{d2} - \beta_{d1} fal(e_d, \alpha_{d1}, \delta_d) + \dfrac{1}{L_d} u_d \\ \dot{z}_{d2} = -\beta_{d2} fal(e_d, \alpha_{d2}, \delta_d) \end{cases} \tag{9}$$

where i_d is actual measured value through coordinate transformation; z_{d1} is estimate of i_d; z_{d2} is estimate of w_d; β_{d1} and β_{d2} are adjustable parameters which are determined by sampling time; $f_d = -\dfrac{R_s}{L_d} i_d$; $w_d = \dfrac{\omega_r L_q}{L_d} i_q$; $f_q = -\dfrac{R_s}{L_q} i_q$;

$$w_d = -\frac{\left(L_d i_d + \varphi_f\right)\omega_r}{L_q}$$

The NLSEF of *d*-axis current is presented by:

$$\begin{cases} \Delta i_d = z_{d1} - i_d^* \\ u_{od} = k_d fal\left(\Delta i_d, \alpha_{0d}, \delta_{0d}\right) \end{cases} \tag{10}$$

where i_d^* is *d*-axis current reference, k_d. is adjustable parameter.

The control input u_d for the IPMSM is expressed as:

$$u_d = L_d\left[u_{0d} - \left(f_d + z_{d2}\right)\right] \tag{11}$$

Substituting (12) into (9) yields

$$\dot{i}_d = u_{0d} \tag{12}$$

The estimator of extended state is fed back to the control input via disturbance compensation which makes *d*-axis current model into a linear integral model. The *q*-axis current regulator is the same with *d*-axis.

III. TRANSITION RULES

When rotor speed is less than or equal to base speed, the back-EMF is always less than the maximum output voltage of the inverter and the MTPA control is chose. When $\omega_r > \omega_c$, the field-weakening control is used. For $\omega_{base} < \omega_r \le \omega_c$, if the back-EMF is less than or equal to U_{sm}, the MTPA control is chose, or else the field-weakening control is chose.

During high speed operation, ω_c is easily varied because of the rotor permanent magnet performance change and the available maximum voltage. Moreover, the voltage of batteries in application for EV has much amplitude of fluctuation. To smooth the transition between both control modes, the voltage of batteries is introduced to determine the choice of control modes combined with the base speed and the output voltage of the ADRC current regulator. The flowchart of the improved transition is shown in Fig. 5.

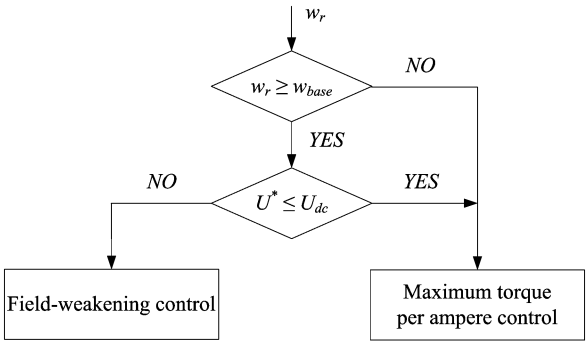

Fig. 2 flowchart of transition of control modes

IV. RESULTS AND DISCUSSIONS

To verify the performances in terms of cross-coupling effects and current regulator saturation, *d*- and *q*-axis responses of the ADRC current regulator in field-weakening region is shown in Fig. 3 when the speed varies from 0 to 3400rpm. The *d*- and *q*-axis current responses can effectively follow the current commands.

The transitions between both control modes in first field-weakening region are shown in Fig. 4. A step speed command of 3400rpm is applied to the IPMSM drive system. The load torque is 1N·m. When the motor is accelerated below the base speed, the MTPA control mode is chosen to produce maximum torque. The corresponding *d*- and *q*-axis currents follow the i_{dm} and i_{qm}. When the motor speed is greater than the base speed, the smooth transition takes place. When the motor speed reaches the command speed 3400rpm and operates steady-state, the transition of control mode occurs again. The MTPA control mode is used.

The ADRC current regulator can timely control the *d*- and *q*-axis currents to provide the maximum torque during

IPMSM acceleration. The transitions between the MTPA control to field-weakening control are smooth.

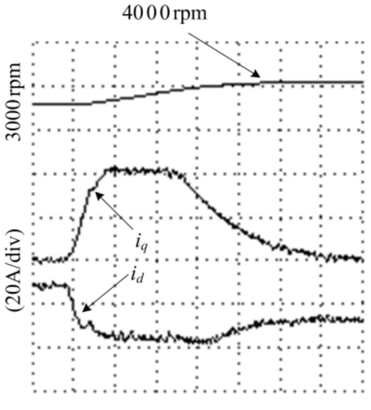

Fig. 3 Results of i_d and i_q, when motor accelerating in field-weakening region.

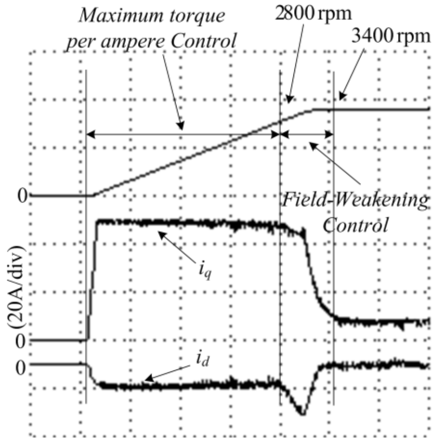

Fig. 4. Results of i_d and i_q, in transition process of control mode under lighter load

V. Conclusion

This paper introduces the high efficiency current control of IPMSM and transition rules. The cross-coupling terms are regarded disturbances and the ADRC is used to estimate the disturbances. The estimators of the disturbances are compensated. The nonlinear current model is converted to linear integrator series one. The linear current model no longer contains the motor parameters such as inductances, stator resistance, electrical angular velocity and flux linkage. The results demonstrate that the ADRC current regulator realizes the desirable performance of the proposed method for wide-speed operation

References

[1] M. Uddin, T. Radwan, M. Rahman, "Performance of interior permanent magnet motor drive over wide speed range," *IEEE Trans. on Energy Conversion*, vol. 17, no. 1, Mar. 2002, pp. 79-84.

[2] T. Noguchi, "Trends of Permanent-magnet Synchronous Machine Drives," *IEEJ Trans. on electrical and electronic engineering*, vol. 2, 2007, pp. 125–142.

[3] C. Cavallaro, A. O. Di Tommaso, R. Miceli, A. Raciti, G. R. Galluzzo, M. Trapanese, "Efficiency enhancement of permanent-magnet synchronous motor drives by online loss minimization approaches," *IEEE Trans. on Industrial Electronics*, vol. 52, no. 4, Aug. 2005, pp. 1153–1160.

[4] J. Lian, Y. Zhou, T. Ma, W. Wang, "Design for motor controller in hybrid electric vehicle based on vector frequency conversion technology," *Mathematical Problems in Engineering*, vol. 2010, Article ID. 627836.

[5] C.T. Pan, S.M. Sue, "A linear maximum torque per ampere control for IPMSM drives over full-speed range," *IEEE Trans. on Energy Conversion*, vol. 20, no, 2, Jun. 2005, pp. 359-366.

[6] S. Morimoto, M. Sanada, Y. Takeda, "Wide-speed operation of interior permanent magnet synchronous motors with high-performance current regulator," *IEEE Trans. on Industry Applications*, vol. 30, no, 4, Jul./Aug. 1994, pp. 920-926.

[7] O. Ojo, F. Osaloni, Z. Wu, M. Omoigui, "A control strategy for optimum efficiency operation of high performance interior permanent magnet motor drives," in Conf. Rec. *IEEE IAS Annu. Meeting*, vol. 1, Oct. 2003, pp. 604-610.

[8] B. Bae, N. Patel, S. Schulz,S. Sui, "New field weakening technique for high saliency interior permanent magnet motor," in Conf. Rec. *IEEE IAS Annu. Meeting*, vol. 2, Oct. 2003, pp. 898-905.

[9] T. Kwon, G. Choi, M. Kwar, S. Sul, "Novel flux-weakening control of an IPMSM for quasi-six-step operation," *IEEE Trans. on Industry Applications*, vol. 44, no. 6, Nov./Dec. 2008, pp. 1722-1731.

[10] J. Kim, S. Sul, "Speed control of interior permanent magnet synchronous motor drive for the flux weakening operation," IEEE Trans. on Industry Applications, vol. 33, no. 1, Jan./Feb. 1997, pp. 43-48.

[11] G. Gabriel, S. Fan, E. James, "Optimum torque control of permanent-magnet AC machines in the field-weakening region," *IEEE Trans. on Industry Applications*, vol. 41, no. 4, Jul./Aug. 2005, pp. 1020-1028.

[12] J.Q. Han, "Auto disturbances rejection control technique," *Frontier Science*, no. 1, 2007, pp. 24-31.

[13] [13] J.Q. Han, "From PID technique to auto disturbance rejection control technique," *Control Engineering of China*, vol. 9, no. 3, May, 2002, pp. 40-45.

[14] J.Q. Han, "Auto-disturbances-rejection controller and its applications," *Contr. Decision*, vol. 13, no. 1, Jan. 1998, pp. 19-23.

Wen Jianping He received the Ph. D. degree in mechanical engineering from Xi'an Jiaorong University. His research interests in the areas of the technology on the control of drive for EV.

Zhang Xuhui His research interests in the areas of intelligent measurement and control and mechanical & electric equipments technical study.